Research Article

Kadri Kurt*

The seasonal variation in the polarization (E_x/E_y) of the characteristic wave in ionosphere plasma

https://doi.org/10.1515/phys-2022-0184
received January 29, 2022; accepted July 03, 2022

Abstract: Light is a well-known electromagnetic wave that propagates, transmits, reflects, and polarizes in any medium. Waves have a huge technical impact as a determinant of human life because of their qualities. Using real geometrical Earth's magnetic field, this article investigates the latitude and seasonal fluctuation of polarization magnitude of a polarized characteristic wave (no electric flux in the wave's propagation direction) in the ionospheric plasma (the examined conditions). Both the volume polarization and wave polarization have been solved analytically in the ionospheric plasma, taking into account the accepted parameters. Furthermore, the volume and wave polarization were mathematically proven to be connected, and numerical wave polarization values were produced in the ionospheric plasma under the considered parameters. When a magnetic field operates on a medium, it causes the medium to become anisotropic. The wave polarization is ecliptic and the electric field vector does not sweep a circle as understood from analytical solutions when the Earth's magnetic field and particle collisions are taken into account. There is a real and an imaginary element to the wave's electric field ratio ($E_x/E_y = a + ib$). The real and imaginary parts of wave polarization in the x and y planes form the shape of the elliptic structure, and the real component is associated with advancing, while the imaginary part is related to attentiveness. The ionosphere of Earth, all physical parameters, such as refractive index, dielectric structure, and conductivity, have a complicated structure. According to the study, the real part of the polarization of the characteristic wave is related to the absorption coefficient and the imaginary part is proportional to the refractive index of the medium.

Keywords: light propagation, light polarization, ionosphere plasma

* **Corresponding author: Kadri Kurt,** Department of Electricity and Energy, Batman University, Beşiri OSB Vocational School, Batman, Turkey, e-mail: kadrikurtt@hotmail.com

1 Introduction

The term "polarization" has two meanings: first, it refers to the dipole moment per unit volume of the medium, and second, it refers to the wave's polarization. When there is a chance of misunderstanding, these will refer to two magnitudes as "volume-polarization" and "wave-polarization," respectively. It is worth noting that the two definitions arose from the same concept of producing opposite polarity at opposite ends of a line, but in quite different ways. The link to volume polarization is self-evident. When it was considered that light was made up of corpuscles in nature, it was proposed that the corpuscles acquired polarity along a certain direction, known as the direction of polarization, to give a better understanding of double refraction. A careful examination of the charge carriers' reactions to the oscillating **E** and **B** fields can reveal a linear relationship between the waves' electric field **E** and polarization **P** [1–20]. Electric currents, conductivities, refractive index and diffusion, propagation and reflection, and other topics connected to the ionosphere have all been studied by various researchers. Theoretical and experimental issues in the ionosphere remain to this day [1–3,6–17,21–24]. However, all of these were commonly employed in ionospheric plasma approximation and under unique circumstances [17–20]. Plasma in the ionosphere is a poor conductor, with its dielectric properties taking precedence. Despite the fact that the ionospheric plasma becomes a weakly conducting fluid, it may exhibit dielectric qualities under certain conditions. Having a conductor property, on the other hand, causes it to reflect waves. In this scenario, it is important to figure out whether an electromagnetic wave sent from the Earth to the ionosphere is inductive or capacitive [9–13]. There are numerous studies in the literature, particularly on the conductivity of ionospheric plasma; however, there are few studies on the volume and wave polarization features of ionospheric plasma. However, the polarization of electromagnetic waves in plasma waves has been explored, as evidenced by research by Budden, Swanson, Ratcliffe, and others [9–16]. Many scientists have worked on certain unique examples related to this topic, and they are continually working on it. Why is studying the polarization of the wave in the ionosphere so important? According to the parameter to be obtained, we would like to know the magnitude and direction of the electromagnetic wave [1,21–24]. In addition, based on the data, we determine the magnitude of the wave polarization to obtain information about the medium. As a result, investigations on the polarization of electromagnetic waves in the ionospheric plasma are insufficient [9–14]. In reality, the polarization wave in any medium determines part of the medium's features and wave behavior. As a result, it is closely related to electromagnetic wave propagation and is critical for ionospheric plasma [1–6,21–24]. It can be stated that the ionosphere has more predominant dielectric properties than its conductivity, but to know the properties of the ionosphere, its conductive properties are used like making of ionosonde [14–17].

The main goal of this research is to establish a relationship between the polarization of charged particles in the medium and the polarization of a radio wave sent outside to the ionosphere medium, to calculate the wave's polarization magnitude under certain conditions, and to investigate the trajectory of the polarization vector.

1.1 Volume polarization tensor for cold ionosphere plasma in northern hemisphere

To begin with, we calculated the volume polarization tensor in ionospheric plasma under cold plasma conditions (P "pressure gradient term" = 0, cold plasma approach) and the magnitudes of volume polarization constants for the accepted parameters as shown in Figure 1. Refs [1–3,21–24] give the ambient magnetic field in the northern hemisphere.

$$\boldsymbol{B} = B_x \boldsymbol{a}_x + B_y \boldsymbol{a}_y + B_z \boldsymbol{a}_z, \tag{1}$$

where $B_x = B_0 \cos I \sin d$, $B_y = B_0 \cos I \cos d$, and $B_z = -B_0 \sin I$. I and d are the magnetic dip and the magnetic declination angles, respectively.

The force acting on an electron in the cold plasma is given by

$$m\frac{\mathrm{d}\ddot{\boldsymbol{r}}}{\mathrm{d}t^2} = -e(\boldsymbol{E} + \dot{\boldsymbol{r}} \times \boldsymbol{B}) - m\nu\dot{\boldsymbol{r}}. \tag{2}$$

where $\boldsymbol{r}$, $\boldsymbol{B}$ and $\boldsymbol{E}$ (= electron-ion + electron-notr collisions frequency) are the position vector, the magnetic field of the Earth, electric field, respectively. Here all of the fields change like $e^{i(\omega t - \mathbf{k}.\mathbf{r})}$. The movement of an electron from point A to point B is equivalent to leaving the original electron undisturbed at A and adding a dipole as shown in Figure 2, so that it cancels the original charge at A.

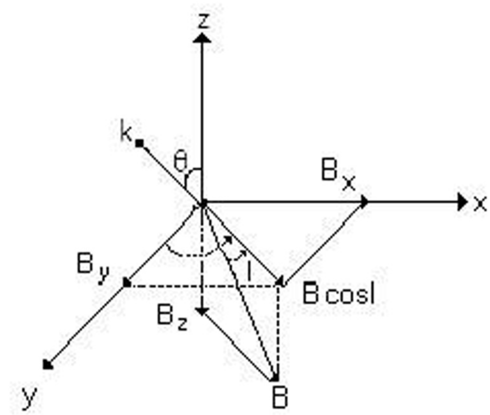

Figure 1: The geometry of Earth's magnetic field for the northern hemisphere [6,21,22].

If there are N electrons per unit volume, and all move through equal distance r, equivalent dipole moment, the volume polarization is given by [1–5]:

$$\boldsymbol{P} = Ne\mathbf{r} = \varepsilon_0 \chi \boldsymbol{E}. \tag{3}$$

The electric field of wave $\boldsymbol{E}$ causes the electrons to flow and the polarization $\boldsymbol{P}$ to occur. $\boldsymbol{P}$ and $\boldsymbol{E}$ are parallel if there is no applied magnetic field; otherwise, $\boldsymbol{P}$ and $\boldsymbol{E}$ are not parallel. When we combine Eqs. (1)–(3), we get volume polarization for the northern hemisphere.

$$(i\omega\nu - \omega^2)P_x - i\omega\omega_{cz}P_y - i\omega\omega_{cy}P_z = \frac{Ne^2}{m}E_x, \tag{4}$$

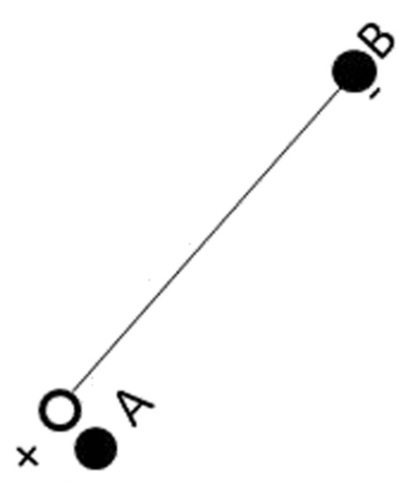

Figure 2: The movement of an electron from A to B is equivalent to the addition of a dipole [5].

$$i\omega\omega_{cz}P_x + (i\omega\nu - \omega^2)P_y - i\omega\omega_{cx}P_z = \frac{Ne^2}{m}E_y, \quad (5)$$

$$-i\omega\omega_{cy}P_x + i\omega\omega_{cx}P_y + (i\omega\nu - \omega^2)P_z = \frac{Ne^2}{m}E_z, \quad (6)$$

The frequency components of the cyclotron are as follows:

$$\omega_{cx} = \frac{eB_x}{m}, \omega_{cy} = \frac{eB_y}{m} \text{ and } \omega_{cz} = \frac{eB_z}{m}.$$

From here

$$\begin{aligned} P_x &= \frac{a[(i\nu\omega - \omega^2)^2 + \omega^2\omega_{cx}^2]}{A + iB}E_x \\ &+ \frac{a[i\omega\omega_{cz}(i\nu\omega - \omega^2) - \omega^2\omega_{cx}\omega_{cy}]}{A + iB}E_y \\ &+ \frac{a[-i\omega\omega_{cy}(i\nu\omega - \omega^2) - \omega^2\omega_{cx}\omega_{cz}]}{A + iB}E_z, \end{aligned} \quad (7)$$

$$\begin{aligned} P_y &= \frac{-a[i\omega\omega_{cz}(i\nu\omega - \omega^2) + \omega^2\omega_{cx}\omega_{cy}]}{A + iB}E_x \\ &+ \frac{a[(i\nu\omega - \omega^2)^2 - \omega^2\omega_{cy}^2]}{A + iB}E_y \\ &+ \frac{a[-i\omega\omega_{cx}(i\nu\omega - \omega^2) - \omega^2\omega_{cy}\omega_{cz}]}{A + iB}E_z, \end{aligned} \quad (8)$$

$$\begin{aligned} P_z &= \frac{a[i\omega\omega_{cy}(i\nu\omega - \omega^2) + \omega^2\omega_{cx}\omega_{cz}]}{A + iB}E_x \\ &+ \frac{a[-i\omega\omega_{cx}(i\nu\omega - \omega^2) - \omega^2\omega_{cz}\omega_{cy}]}{A + iB}E_y \\ &+ \frac{a[(i\nu\omega - \omega^2)^2 - \omega^2\omega_{cz}^2]}{A + iB}E_z, \end{aligned} \quad (9)$$

where constant coefficients

$$A = \omega^2(\nu^2 + \omega^2(1 + \omega_c^2)),$$
$$B = \omega\nu(\nu^2 - \omega^2\omega_c^2) \text{ and } a = \frac{Ne^2}{m}.$$

If all the volume polarization coefficients are rearranged for both real and imaginary, P_x, $P_{y,}$ and P_z are obtained as follows.

$$P_x = (\alpha_{11R} - i\alpha_{11I})E_x + (\alpha_{12R} + i\alpha_{12I})E_y + (\alpha_{13R} + i\alpha_{13I})E_z, \quad (10)$$

$$P_y = (\alpha_{21R} + i\alpha_{21I})E_x + (\alpha_{22R} - i\alpha_{22I})E_y + (\alpha_{23R} - i\alpha_{23I})E_z, \quad (11)$$

$$P_z = (\alpha_{31R} - i\alpha_{31I})E_x + (\alpha_{32R} + i\alpha_{32I})E_y + (\alpha_{33R} - i\alpha_{33I})E_z. \quad (12)$$

Volume-polarization tensor could be obtained depending on the permittivity coefficient (χ) as follows:

$$\begin{pmatrix} P_{(x)} \\ P_{(y)} \\ P_{(z)} \end{pmatrix} = \varepsilon_0 \begin{pmatrix} \chi_{11} & \chi_{12} & \chi_{13} \\ \chi_{21} & \chi_{22} & \chi_{23} \\ \chi_{31} & \chi_{32} & \chi_{33} \end{pmatrix} \begin{pmatrix} E_x \\ E_y \\ E_z \end{pmatrix}. \quad (13)$$

The coefficients in Eqs. (10)–(12) are as follows:

$$\alpha_{11R} = \frac{Aa[\omega^2(\omega^2 + \omega_{cx}^2 - \nu^2)] - 2Ba\nu\omega^3}{A^2 + B^2},$$
$$\alpha_{11I} = \frac{[Ba\omega^2(\omega^2 + \omega_{cx}^2 - \nu^2)] - 2Aa\nu\omega^3}{A^2 + B^2},$$

$$\alpha_{12R} = \frac{-Aa[\omega^2(\nu\omega_{cz} + \omega_{cx}\omega_{cy})] - Ba\omega_{cz}\omega^3}{A^2 + B^2},$$
$$\alpha_{12I} = \frac{[Ba\omega^2(\nu\omega_{cz} + \omega_{cx}\omega_{cy})] - Aa\omega_{cz}\omega^3}{A^2 + B^2},$$

$$\alpha_{12R} = \frac{-Aa[\omega^2(\nu\omega_{cz} + \omega_{cx}\omega_{cy})] - Ba\omega_{cz}\omega^3}{A^2 + B^2},$$
$$\alpha_{12I} = \frac{[Ba\omega^2(\nu\omega_{cz} + \omega_{cx}\omega_{cy})] - Aa\omega_{cz}\omega^3}{A^2 + B^2},$$

$$\alpha_{12R} = \frac{-Aa[\omega^2(\nu\omega_{cz} + \omega_{cx}\omega_{cy})] - Ba\omega_{cz}\omega^3}{A^2 + B^2},$$
$$\alpha_{12I} = \frac{[Ba\omega^2(\nu\omega_{cz} + \omega_{cx}\omega_{cy})] - Aa\omega_{cz}\omega^3}{A^2 + B^2},$$

$$\alpha_{22R} = \frac{Aa[\omega^2(\omega^2 - \nu^2 - \omega_{cy}^2)] - 2Ba\nu\omega^3}{A^2 + B^2},$$
$$\alpha_{22I} = \frac{[Ba\omega^2(\omega^2 - \nu^2 - \omega_{cy}^2)] + 2Aa\nu\omega^3}{A^2 + B^2},$$

$$\alpha_{23R} = \frac{-Aa[\omega^2(\nu\omega_{cx} + \omega_{cy}\omega_{cz})] - Ba\omega_{cx}\omega^3}{A^2 + B^2},$$
$$\alpha_{23I} = \frac{[Ba\omega^2(\nu\omega_{cx} + \omega_{cy}\omega_{cz})] - Aa\omega_{cx}\omega^3}{A^2 + B^2},$$

$$\alpha_{31R} = \frac{-Aa[\omega^2(\nu\omega_{cy} + \omega_{cx}\omega_{cz})] - Ba\omega_{cy}\omega^3}{A^2 + B^2},$$
$$\alpha_{31I} = \frac{[Ba\omega^2(\nu\omega_{cx} + \omega_{cy}\omega_{cz})] - Aa\omega_{cy}\omega^3}{A^2 + B^2},$$

$$\alpha_{31R} = \frac{-Aa[\omega^2(\nu\omega_{cy} + \omega_{cx}\omega_{cz})] - Ba\omega_{cy}\omega^3}{A^2 + B^2},$$
$$\alpha_{31I} = \frac{[Ba\omega^2(\nu\omega_{cx} + \omega_{cy}\omega_{cz})] - Aa\omega_{cy}\omega^3}{A^2 + B^2},$$

$$\alpha_{33R} = \frac{Aa[\omega^2(\omega^2 - \nu^2 - \omega_{cz}^2)] - 2Ba\nu\omega^3}{A^2 + B^2},$$
$$\alpha_{33I} = \frac{[Ba\omega^2(\omega^2 - \nu^2 - \omega_{cz}^2)] + 2Aa\nu\omega^3}{A^2 + B^2}.$$

2 The wave polarization tensor of characteristic wave in the cold ionospheric plasma for northern hemisphere

The electric flux ($\boldsymbol{D}$) of any medium is given by a well-known equation as follows [1–17]:

$$\boldsymbol{D} = \varepsilon_0 \boldsymbol{E} + \boldsymbol{P}. \tag{14}$$

The characteristic wave's electric flux cannot exist in the propagation direction. When this condition is utilized in Eqs. (11)–(13), as a result $D_z = 0$. The polarization coefficients are derived by

$$P_x = (\mu_R + i\mu_I)E_x + (\sigma_R + i\sigma_I)E_y, \tag{15}$$

$$P_y = (\rho_R + i\rho_I)E_x + (W_R + iW_I)E_y, \tag{16}$$

$$\frac{P_x}{P_y} = \frac{E_x}{E_y}. \tag{17}$$

When Eqs. (16)–(18) are used together, the equation of the characteristic wave is as follows:

$$\left(\frac{E_x}{E_y}\right)_{1,2} = \frac{-(K_R + iK_I)}{2(\rho_R^2 + \rho_I^2)} \mp \frac{\sqrt{K_{1R} + iK_{1I}}}{2(\rho_R^2 + \rho_I^2)}. \tag{18}$$

We could write the expression in square root after mathematical manipulation as follows:

$$\sqrt{K_{1R} + iK_{1I}} = \sqrt{K_{1R}^2 + K_{1I}^2} \times \left[\cos\left(\frac{\theta + 2k\pi}{n}\right) + i\sin\left(\frac{\theta + 2k\pi}{n}\right)\right],$$
$$n = 2 \text{ and } k = 0, 1.$$

3 Numerical analysis and results

Eq. (18) was used to compute the wave polarization for the characteristic wave at hours 12.00–24.00 LT for the year 1990 as seasonal. The IRI model was utilized to calculate the ionospheric parameters that were employed in the calculations. For the characteristic wave in the ionospheric plasma, we evaluated the seasonal change in Eq. (18) about latitude for 12.00 and 24.00 LT at 230 km altitude (F-region). The most essential property of the characteristic wave is that the polarization direction of the wave cannot change while it travels through any medium, making it necessary to make some parallel approaches. Furthermore, there is no induced magnetic polarization matching to electric polarization, and the electric flux does not occur in the wave's progress direction. In the z-direction, there is no electric flow, and the current density and the electric field are not in phase. We achieved the following findings for the corresponding conditions. The change in latitude of the component of real and imaginary at Eq. (15) at 12.00 LT for an altitude of 230 km is shown in Figure 3(a and b) (this altitude is the beginning altitude of F2 peak, "which is the region where the maximum electron density occurs in the ionosphere"). The variation in the real part of wave polarization $(E_x/E_y)_R$ with latitude has been shown in Figure 3. When the variation in the real parts of wave polarization with latitude is analyzed, the real part of wave polarization shows the same tendency for all seasons, according to it. It has greatest values in −75°S and 75°N latitudes, and minimum values at −60°S and 30°N latitudes. We can deduce that the real part of a

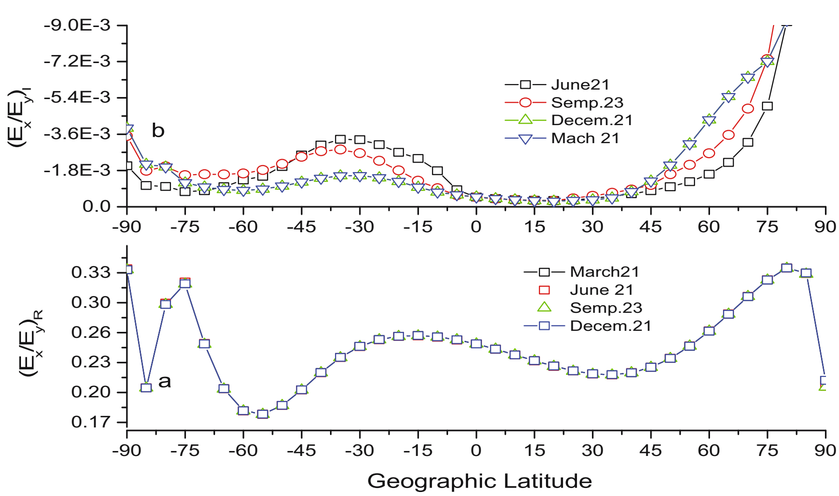

Figure 3: Seasonal change in the (a) real and (b) imaginary components of the polarized wave with latitude (12.00 LT).

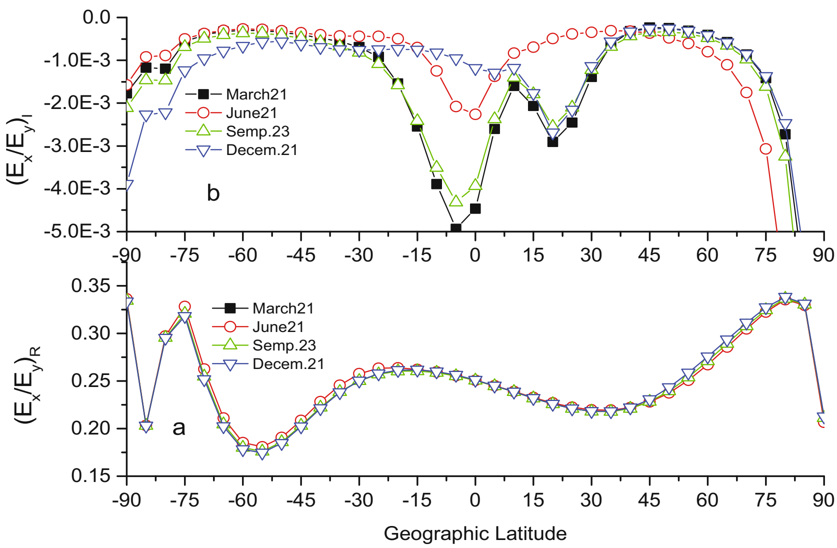

Figure 4: Seasonal change in the (a) real and (b) imaginary components of the polarized wave with latitude (24.00 LT).

characteristic wave's polarization has a seasonal harmonic behavior, with a magnitude equal to the order of magnitude of the refractive index [1,23]. However, there has been little to no change. The imaginary component of Eq. (18) has been shown to alter with latitudes in Figure 3b. Its maximum and minimum values differ from those in Figure 3a. So, the imaginary part of the characteristic wave polarization coefficient has greater values on June 21 (the period when electron density is highest) than in other seasons. We may deduce that the real part of the polarization characteristic wave has been taking larger values at high latitudes for the entire season, but that these values have been dropping especially for north latitudes, and that these values have been minimum between 0 and 45°N latitudes for all seasons. Similarly, the imagined part has been a tendency for all seasons. Unlike the real part, it has various values for 12.00 LT in each season. The latitude of both the real and imaginary parts of the polarization of the characteristic wave for 24.00 LT is shown in Figure 4a and b. In fact, the change in the real part with latitude in Figure 4a is similar to the change in the real part at 12.00 LT for all seasons. They are using the same latitudes for the maximum and minimum. The values at 24.00 LT, on the other hand, are slightly higher.

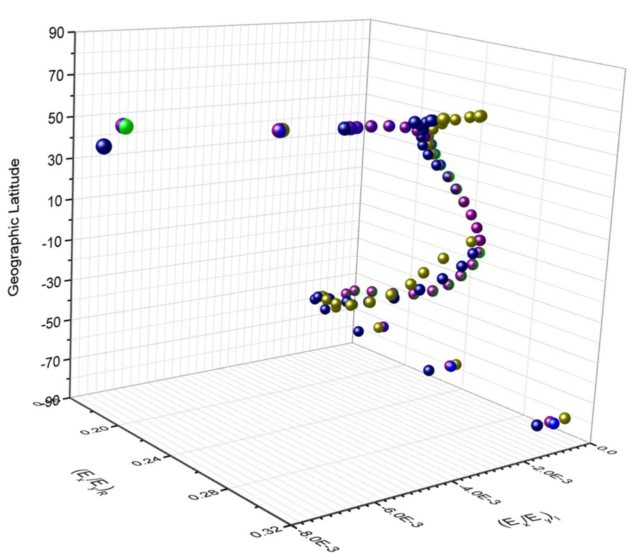

Figure 5: The 3D diagram of characteristic wave polarization (12.00 LT).

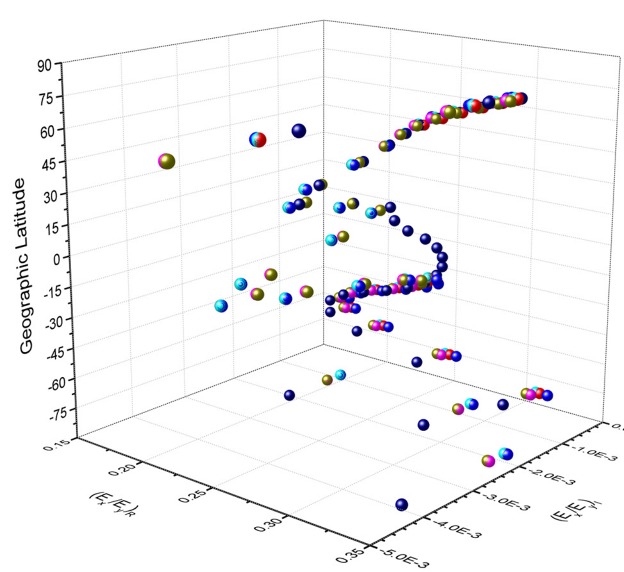

Figure 6: The 3D diagram of characteristic wave polarization (24.00 LT).

For all seasons, the fluctuation of the imaginary part of the polarization of the characteristic wave with latitude at 24.00 LT *vs* 12.00 LT is interesting. In latitudes near the equator, especially at low latitudes, there are significant declines. On March 21st, the most severe reduction happens, and on June 21st, the least. Other middle and high latitudes have similar changes to 12.00 LT. It is possible that this is related to a change in electron density. Because, whatever happens, electron density is the most important component of the ionosphere. The characteristic wave is depicted in three dimensions in Figure 5. The real part is represented by the x-axis, the imaginary part by the y-axis, and geographic latitude is represented by the vertical axis. The electric field vector is considered to be capable of rotating around the z-axis, as seen in Figure 5 and Eq. (7). The characteristic wave's electric field vector is bigger at high latitudes, smaller at medium latitudes, and smallest at low latitudes. This situation could be explained as follows. The precipitation of electrons flowing from south to north along the magnetic field encircling the Earth can cause the electric field vector strength of the upper latitudes to increase.

4 Conclusion

Using the real geometry of the Earth's magnetic field in the northern hemisphere, this study analyzes the amplitude of characteristic wave polarization of $D_z = 0$ for all seasons. In some ways, the outcomes are as expected, but in others, they are absolutely startling. The polarization is elliptic when the Earth's magnetic field is taken into consideration, and the electric field vector does not sweep a circle. It also exhibits a harmonic characteristic, as shown in Figures 5 and 6. This is not surprising in theory. However, it is interesting to note that towards high latitudes, both the real and imaginary parts have high values. The major parameter of the ionosphere, without a question, is electron density. Electron density, on the other hand, is greatly influenced by the ionosphere's external dynamics (such as solar radiation) as well as its internal dynamics (like chemical reactions). We can deduce that this scenario is caused by polar electron precipitation. Winter has a bigger size of the imaginary part of the characteristic wave polarization than summer at 24.00 LT. It has to do with aberrant electron density behavior. The more the atoms and molecules in the atmosphere ionize, the more the Sun's rays reach the Earth's surface in summer than in winter. The number of electrons is projected to increase greater in the summer than in the winter. In the winter, however, the electron density is larger than in the summer. This could be due to an anomaly. This anomaly is explained by the imaginary component of the magnitude of polarization coefficients. Finally, the findings are consistent with previous research.

Funding information: The author states no funding involved.

Author contributions: The author has accepted responsibility for the entire content of this manuscript and approved its submission.

Conflict of interest: The author states no conflict of interest.

References

[1] Sagir S, Yesil A. The relation between the refractive index of the equatorial ionospheric F2 region and long-term solar indices. Wirel Pers Commun. 2018;102(1):31–40.
[2] Yesil A. The effect of the cold plasma on the propagation of the electromagnetic waves. Master thesis. Elazig: Firat University; 1995.
[3] Yesil A. The effect of the electron temperature on the electric polarization coefficient of ionospheric plasma. Int J Sci Tech. 2006;1(2):125–30.
[4] Kaladze T, Tsamalashvili L, Kaladze D, Ozcan O, Yesil A, Inc M. Modified KdV equation for magnetized Rossby waves in a zonal flow of the ionospheric E-layer. Phys Lett A. 2019;383(32):125888.
[5] Ratcliffe JA. The magneto-ionic theory and its applications to the ionosphere. London: Cambridge University Press; 1959.
[6] Timucin E, Unal I, Yesil A. The Effect of the midlatitude electron density trough on the ionospheric conductivities. Iran J Sci Technol Trans A Sci. 2019;43(1):297–07.
[7] Yesil A, Kurt K. Calculation of electric field strength in the ionospheric F-region. Ther Sci. 2019;22(Suppl. 1):159–64.
[8] Timocin E, Yesil A, Unal I. The effect of the geomagnetic activity to the hourly variations of ionospheric foF2 values at low latitudes. Arab J Geosci. 2014;7(10):4437–42.
[9] Swanson DG. Plasma waves. New York: Academic Press; 1989.
[10] Whitten RC, Popoff IG. Fundamentals of aeoronmy. New York: John Willey and Sons; 1971.
[11] Budden KG. The propagation of radio waves. Cambridge: Cambridge University Press; 1988.
[12] Budden KG, Stott GF. Rays in magneto-ionic theory-II. J Atmos Sol-Terr Phys. 1980;42:791–800.
[13] Richard F. The physics of plasma. New York: CRC Press; 2014. p. 50–140.
[14] Hunsucker RD, Hargreaves JK. The high-latitude ionosphere and its effects on radio propagation. United Kingdom: Cambridge University Press; 2003. p. 1–50.
[15] Rishbeth H. Physics and chemistry of the ionosphere. Contemp. Phys. 1973;14(3):229–49.
[16] Rishbeth H, Garriot OK. Introduction to ionospheric physics. New York: Academic Press; 1969.

[17] Sağir S, Yaşar M, Atici R. The Relationship between Dst, IMF-Bz and collision parameters for $O + N_2 \rightarrow NO^+ + N$ reactive scattering in the Ionosphere. Geomagn Aeron. 2019;59:1003–8.
[18] Yasar M. The solar eclipse effect on diffusion processes of $O^+ + O_2 \rightarrow O_2^+ + O$ reaction for the upper ionosphere over Kharkiv. Therm Sci. 2021;25(1):57–63.
[19] Yasar M. The change of diffusion processes for $O + N_2 \rightarrow NO^+ + N$ reaction in the ionospheric F region during the solar eclipse over Kharkiv. Therm Sci. 2021;25(1):51–6.
[20] Yasar M. Investigation of ionospheric losses for the $O^+ + O_2 \rightarrow O_2^+ + O$ reaction during the solar eclipse. Phys Scr. 2021;96(9):094011.
[21] Unal I, Senalp ET, Yeşil A, Tulunay Y, Tulunay E. Performance of IRI-based ionospheric critical frequency calculations concerning forecasting. Radio Sci. 2011;46(1):1–10.
[22] Yesil A, Sagir S, Kurt K. The Behaviour of the classical diffusion tensor for equatorial ionospheric plasma. J Sci. 2016;13:123–7.
[23] Yesil A, Unal I. Electromagnetic wave propagation in ionospheric plasma, in A. Akdagli (ed.), Behaviour of electromagnetic waves in different media and structures. London: IntechOpen; 2011. doi: 10.5772/19197.
[24] Yesil A, Sagir S. Updating conductivity tensor of cold and warm plasma for equatorial ionosphere F2-region in the northern hemisphere. Iran J Sci Technol Trans A Sci. 2019;43(1):315–20.